Properties of Axicon Systems for Collecting Foil-Excited Accelerator Beam Spectra[*]

John O. Stoner, Jr.

Department of Physics, University of Arizona, Tucson, Arizona 85721

NGR-03-002-017

Abstract

We describe properties of a particular kind of light-collecting system used for spectroscopy of light emitted by foil-excited accelerator beams. This system, built to test the possibility of obtaining narrow lines from such sources, has as its basic optical element an axicon, a conical reflector with its axis coincident with that of the accelerator beam. We consider the properties of an axicon followed by a lens and aperture and point out some criteria which are appropriate to the design of optical systems using such devices. Experimentally we find that scattering of the accelerator beam by the foil contributes significantly to spectral linewidths.

Introduction

We have used an axicon for collecting light from foil-excited accelerator beams. This device, which was used to test the possibility of obtaining narrow spectral lines from foil-excited accelerator beam sources, has properties which in some circumstances make its use appropriate for the study of spectral line shapes and structures. We describe here some of these properties and indicate some of the advantages and limitations of axicon-based optical systems. We find that scattering of the beam by the foil often limits the reduction of linewidths obtainable with this mode of observation.

Optical Properties

We assume throughout the following that the accelerator beam radiates isotropically, and that the reduction of excited ion density due to decays is unimportant. The latter assumption (which often holds in practice) makes possible a simplified analysis in which many of the essential properties of axicon collection systems are easily displayed. A detailed analysis of the effects of finite ion state lifetimes is not included here.

Axicon optical elements were first discussed in detail by McLeod.[1] The original suggestion[2] and subsequent development[3] of this technique for collecting light from electronically-excited ion beams involve the optical system shown in Fig. 1 (see also Ref. 3). The axicon, a conical reflector with its optic axis coincident with the accelerator beam axis, collects light emitted into a small range of angles about perpendiculars to the beam and

directs it into a small range of angles about parallels to the beam. We will usually assume that the foil is located at the projected apex of the axicon and that the axicon is a perfectly-reflecting hollow cone with 90° total apex angle. Some of the characteristics of solid axicons (which use total internal reflection at the conical surface) will be mentioned later. The circular aperture S is located in the focal plane of lens L, and restricts the light transmitted to a spectrograph or spectrometer to that leaving the axicon within angle Θ of the optic axis. The light reflected into that angular range by an area element dA of the axicon surface originates in the beam within a cone of half-angle Θ centered on the beam normal through dA (Fig. 2).

For sufficiently small accelerator beam diameters, this system provides complete collection of all light emitted by the beam within the axicon, in the angular range $\pm \Theta$ centered on the beam normal. We will always assume $\Theta \ll 1$ radian. If the beam within the axicon is perfectly collimated, the total width of a spectral line due to this finite angular range of observation is approximately

$$\delta\lambda \doteq 2 \ \beta\Theta\lambda_o \ (1 - \beta^2)^{-1/2} \sim 2 \ \beta\Theta\lambda_o \quad , \tag{1}$$

where $\beta = v/c$ assumed $\ll 1$, v = beam particle speed, c = speed of light, λ_o = wavelength emitted in the ions rest frame. Typical values of β may range from 2×10^{-3} (0.5 MeV U^{238}) to 4.6×10^{-2}

(1.0 MeV H). The requirement on beam diameter (t) for complete light collection in the desired angular range at some point along the excited ion beam is

$$t \ll 2 \; R\Theta$$

where R = axicon radius at that point. For $\delta\lambda = 1\text{Å}$, $\lambda_o = 5000\text{Å}$, $\beta = 10^{-2}$ and R = 1 cm, this implies $\Theta = 10^{-2}$ radian, and t << 0.2 mm. R varies from some minimum value set by the beam stop to some maximum value R_o.

If the ion beam diameter is made comparable to or larger than (2 RΘ), while maintaining uniform ion beam density, the light collection efficiency in the desired angular range is reduced below unity. This is the usual case in practice. The average collection efficiency (η) for the desired light in the case where

$$t \gg 2R\Theta \; , \tag{2}$$

can be found from a simple geometrical construction to be

$$\eta \doteq 2 \; \frac{R\theta}{t} \; .$$

Although the collection efficiency varies along the ion beam and may be far less than unity, the total wavelength spread for light

transmitted through aperture S is given by Eq. (1). The amount
of light collected by S is approximately proportional to beam
thickness t, since the number of excited ions is proportional to
t^2 and η varies nearly as t^{-1}.

In order to find the spectral distribution (irradiance)
of light passing through S, for beams having sufficiently large
diameter that Eq. (2) holds, it is convenient to decompose into
components α and φ the angle θ which an emitted ray reflected
from the axicon makes with a parallel to the beam axis. Only
rays having $\theta \leq \Theta$ pass through the aperture S. In the plane
containing one such emitted ray and the emitting ion's path
(parallel to, but not in general coincident with the beam axis),
the ray makes angle α with the normal to the ion's path (Fig. 2).
The observed wavelength λ is determined by this angle and is
closely

$$\lambda = \lambda_o (1 + \alpha\beta)(1 - \beta^2)^{-1/2} .$$

Projected into a plane perpendicular to the ion's path, the ray
makes an angle φ with the normal through dA (Fig. 2). We then
have approximately that

$$\theta^2 = \alpha^2 + \varphi^2 .$$

The spectral distribution of light in the focal plane of
lens L is found by considering the wavelength distribution of

the light arriving at the axicon in the hollow cone having out-side half-angle $\theta + d\theta$ and inside half-angle θ. The wavelength of a ray contained in the hollow cone depends only on the α component of θ. We assume that a constant beam thickness contributes the light arriving in that hollow cone; then $I_\theta(\Delta\lambda)$, the distribution of wavelength shifts in the emerging light, has the same algebraic form as the distribution of θ values. Using M = number of decays per unit volume per second in the ion beam, and considering an axicon having maximum radius R_o and comparatively small minimum radius (so that we may assume that all parts of the lens are illuminated), we obtain

$$I_\theta(\Delta\lambda)\; d(\Delta\lambda)\; d\theta \doteq \frac{MR_o^2 t}{2} [\beta^2\theta^2\lambda_o^2 (1-\beta^2)^{-1} - (\Delta\lambda)^2]^{-1/2} \theta\; d\theta\; d(\Delta\lambda)$$

$$(3)$$

for $|\Delta\lambda| \leq \beta\theta\lambda_o (1 - \beta^2)^{-1/2}$, and otherwise $I_\theta(\Delta\lambda) = 0$; where $\Delta\lambda$ is the shift in wavelength relative to the value on the beam normal:

$$\Delta\lambda \equiv \lambda - \lambda_o (1 - \beta^2)^{-1/2} .$$

The dimensions of $I_\theta(\Delta\lambda)$ are photons/(time wavelength angle).

For light passing through a circular aperture having angular diameter 2Θ the total spectral distribution is then found by integrating Eq. (3) over θ:

$$I(\Delta\lambda)\, d(\Delta\lambda) = \left[\frac{MR_o{}^2 t(1-\beta^2)}{2\beta^2 \lambda_o{}^2} \right] \left[\beta^2 \Theta^2 \lambda_o{}^2 (1-\beta^2)^{-1} - (\Delta\lambda)^2 \right]^{1/2} d(\Delta\lambda) \quad (4)$$

for $|\Delta\lambda| \leq \beta\Theta\lambda_o(1 - \beta^2)^{-1/2}$; and otherwise $I(\Delta\lambda) = 0$ (Fig. 3).
The dimensions of $I(\Delta\lambda)$ are photons/(time wavelength). The wave-
length dependence of $I(\Delta\lambda)$ is identical to that obtained by
Marquet[2] for the line profile obtained with a more conventional
light-collecting method (assuming $\beta \ll 1$).

The integrated photometric brightness B at S (in photons/
sec-cm^2-sterad) can be found by integrating Eq. (4) and dividing
by the appropriate area and solid angle factors. The result is

$$B = \frac{Mt}{4\pi} \, ,$$

which assumes that Eq. (2) is satisfied and losses are neglected.
This value is equal to the maximum possible brightness obtainable
from the accelerator beam in directions perpendicular to the
beam axis. In optical systems such that a lens images the beam
onto a slit or other aperture, this brightness is obtained only
in the center of the image (where the effective thickness of the
beam is t) and not in the sides of the image.

If the slit of a spectrometer or astigmatic spectrograph is
placed at S, the spectral lines observed at the output have widths
which depend on the choice of slit length as well as slit width
(and which may be roughly constant along the line images). If a
stigmatic spectrograph is used in this fashion, the spectra are
qualitatively different. The light passing through the ends of

the slit has a distribution given by Eq. (3) peaked at the extreme
wavelengths $\lambda_o (1 \pm \beta\theta)(1 - \beta^2)^{-1/2}$. The light passing through the
center of the slit is unbroadened in this ideal case. The result
is the formation of x-shaped "lines", whose brightnesses in their
exact centers in the spectrograph image plane are the same as at
the center of the entrance slit, ignoring spectrograph losses,
and the lines broaden and split toward the ends of the slit
images. Because of the high peak brightnesses obtainable with
this arrangement, there is some prospect of making practical use
of this system; however, the effects of beam scattering by the
foil (c.f. next section) will presumably limit the performances
of such systems.

Effects of Scattering

The light collected by an axicon surrounding an ion beam
is altered significantly when the beam is scattered in the foil
and spreads instead of maintaining constant cross section.
Since we understand only partially the processes leading to
electronic excitation when an ion passes through a carbon foil,
and the processes leading to beam spreading are difficult to
treat accurately, it is not possible at this time to develop
exact expressions for linewidths and intensities for ion beams
excited in this way. The problem of predicting a spectrum collected
by an axicon is compounded by the facts that the collection efficiency
of an axicon varies with axicon and beam diameter, and the number
of excited beam particles per unit length diminishes as they move

downstream. There is also the possibility that the ions might radiate anisotropically.

Scattering affects the spectra obtained by an axicon in two obvious ways: (a) the excited ions move away from their original paths so that the collection efficiency of the axicon diminishes and the intensity of collected light diminishes; (b) the ions obtain velocity components in the line of sight (perpendicular to the ion beam axis) so that the spectral lines are broadened further. Some of the effects of beam scattering in reducing spectroscopic resolution have been discussed by others.[5] We assume for the purposes of discussion that the ion beam is perfectly collimated before it strikes the foil and that the scattering and excitation processes are independent; we continue to neglect changes in the number of decays per unit length as the emitters move downstream.

Multiple scattering in the foil gives rise to a gaussian distribution of ion exit velocities along a direction perpendicular to the beam axis, so long as an ion's energy loss in the foil is not comparable to E, the ion energy. The width of the distribution depends on foil thickness (x), number density (N), atomic number (Z), ion atomic number (z), and ion energy. Elementary considerations[6] yield for the rms scattering angle Ω along a direction perpendicular to the beam:

$$\Omega^2 = \left(\frac{\pi\, Nx\, Z^2 z^2 e^4}{E^2}\right) \ln\left[\frac{a_o E}{Z^{4/3} e^2 z}\right] \tag{5}$$

where a_o = Bohr radius, e = electronic charge. This formula neglects reduced-mass effects which are usually unimportant for hydrogen beams, but may be significant for beams of heavier ions. For 100 keV protons passing through 5 $\mu g/cm^2$ carbon foils, the formula yields Ω = .018 radian; for 250 keV O^+ ions passing through 5 $\mu g/cm^2$ carbon foils the formula yields Ω = .053 radian.

The wavelength distribution $I_s(\Delta\lambda)$ expected from multiple scattering considerations alone is

$$I_s(\Delta\lambda)\ d(\Delta\lambda)\ =\ (\text{constant})\ \exp\left[-\frac{(\Delta\lambda)^2}{2\beta^2\Omega^2\lambda_o^2}\right] d(\Delta\lambda)\ . \qquad (6)$$

The total flux through the aperture S will be appreciably reduced due to scattering at the foil if the effective beam diameter is noticeably increased, since the integrated brightness at S is thereby reduced. The condition to be satisfied for the diameter to be appreciably increased is

$$\Omega\,R_o\ \approx\ t$$

where t represents the initial beam diameter. For lifetime measurements and other photometric measurements in which constant light-collection efficiencies are required, the appropriate criterion is

$$\Omega\,R_o\ \ll\ t\ .$$

The spectral distribution of the light passing through S is broadened by the spreading of the ion beam. We may expect to observe this effect when the ion velocities in the direction of observation due to scattering become comparable to those due to the finite size of the aperture S, or when

$$\Omega \approx \Theta \; .$$

Both effects (i.e., beam size and velocity distribution) cause increased degradation of spectral lines as foil thickness is increased, if other parameters remain constant. The effects have been observed experimentally (Fig. 4). These data, taken by pressure-scanning a Fabry-Perot interferometer fed by light from an axicon, show indications of practical limits on the reduction of linewidths in beam-foil sources. We note that for the hydrogen Balmer lines H_β and the O II lines investigated, the full widths at half maximum (about $2.5\mathring{A}$ and $2\mathring{A}$ respectively) are less than would have been expected (about $5\mathring{A}$ and $2.5\mathring{A}$ respectively) from simple multiple scattering considerations alone (see Eqs. (5) and (6)).

The line shape for light transmitted by S can be found by performing the convolution of Eq. (4) with Eq. (6). For the sake of convenience we generally assume that the widths due to the two causes of broadening add in quadrature, so that the net line-width characteristic of the source, Γ_s, at one-half maximum is approximately equal to

$$\Gamma_s \approx \beta\lambda_o(8\Omega^2 + 4\Theta^2)^{1/2} \ .$$

(The profile of the recorded signal can often be assumed to be
represented by the convolution of the source spectrum with an
instrumental response function having width Γ_i, in which case we
can approximate the observed signal width Γ as

$$\Gamma^2 \doteq \Gamma_s{}^2 + \Gamma_i{}^2 \ .)$$

Since Ω varies approximately as β^{-2}, for a given foil thickness
there will be an ion beam energy for which the linewidth is a
minimum. Experimental indications of this effect are shown in
Fig. 5. Although qualitatively the observed effects of scatter-
ing are well explained, we have observed that the broadening due
to this mechanism is often less than predicted by Eq. (5) (Fig.
6). This leads us to believe that Eq. (5) often seriously over-
estimates the average scattering angle. Other investigators[7]
have come to this conclusion, attributing their results to break-
down of the assumption that multiple scattering is the dominant
process. Shielding of the projectile ion nuclei by electrons in
the foil, and the stabilizing effects of the different parts of a
molecular ion upon one another in the neighborhood of the foil,
may also be responsible for the small widths observed. Detailed
calculations[8] will presumably be necessary for quantitative pre-
dictions of linewidths.

Design Considerations

The essential problem involved in matching an axicon to a spectroscopic instrument is usually that of choosing axicon and beam parameters to optimize the use of an existing instrument. Because for any given experiment there are many parameters which can be varied at will (e.g., beam collimation, particle speed, foil atomic number, spectroscopic resolving power, axicon length), and parameters having fixed values which may differ among ions or levels (e.g., average scattering angle, state lifetimes), it is not possible to provide absolute criteria for designing all such experimental systems.

Some quantities can, however, be chosen a priori. Since scattering in the foil degrades both intensity and linewidth, foil thickness and atomic number should be minimized. Except in cases where the details of the scattering process are to be studied, there is no point in reducing Θ far below Ω, since much light is lost thereby without proportional decrease in linewidth. For the study of a particular transition, little is gained by making the axicon length ($\doteq$ radius R_o) appreciably greater than the product of particle speed and mean life of upper level.

Although the axicon which we have used for these investigations was cut from a piece of fused silica (Fig. 1), we have found that this method of construction is generally not desirable. It is simpler and less expensive to machine the item from metal as a hollow cone. A highly reflecting surface can be produced in the machining process or by vacuum evaporation later. The solid

axicon, using total internal reflection at the conical surface, has several disadvantages associated with the cylindrical bore: it fluoresces if the scattered accelerator beam strikes it; the circular cross section provides undesirable focusing properties (although the shapes of the distributions (3) and (4) are not affected greatly), and if it does not have uniform diameter it can introduce additional Doppler shifts and/or broadening.

- For the usual grating or interferometric analyzers, the product of luminosity (etendue, or light-gathering power)[9] and resolution (wavelength/linewidth) is nearly independent of re-solving power for resolutions less than the maximum attainable. This product for an axicon source is roughly

$$\text{(luminosity)(resolution)} \approx \pi^2 R^2 \Theta^2 \cdot (2\beta\Theta)^{-1} = \frac{\pi^2 R_o^2 \Theta}{2\beta} ,$$

proportional to linewidth. For a particular beam speed and de-sired linewidth (proportional to Θ), it is often possible to choose the axicon radius sufficiently large to fill the entrance optics of any practical analyzing instrument. The useful axicon radius R_o may be limited in some cases by the decay length of the radiation of interest, or the sizes of available optical components.

With an axicon system the integrated brightness in the plane of the aperture S is equal to the maximum possible brightness ob-tainable from the accelerator beam in directions perpendicular to the beam axis. This fact, and the ease of fixing the linewidth

in part by the size of S, constitute the principal advantages of this system. Because of the greater effective source thickness available, end-on viewing of the accelerator beam might yield greater effective source brightness. Some of the advantages of such systems have been described.[10] In order to study the excitation process in foil-excited accelerator beams we have used a Fabry-Perot interferometer, in conjunction with either interference filters or a small grating monochromator to isolate individual spectral lines. With this apparatus it has been desirable to avoid large energy-dependent wavelength shifts; it has been essential to avoid spectral continua (which can arise from fluorescence at the foil and at surfaces struck by the beam). For these purposes an axicon-based optical system has been satisfactory, while extra care would have been necessary in end-on systems to avoid these difficulties. We have had the further advantage that the circular axicon exit aperture S is easily matched optically to the circular entrance aperture of a pressure-scanned interferometer.

References

1. J. H. McLeod, J. Opt. Soc. Amer. 44, 592 (1954).

2. A. B. Meinel, (private communication to S. Bashkin).

3. S. Bashkin, Ed., Proceedings of the Conference on Beam Foil Spectroscopy (Gordon and Breach, New York, 1968), pp. 3-43 S. Bashkin, Appl. Opt. 7, 2341 (1968).

4. L. C. Marquet, J. Opt. Soc. Amer. 57, 878 (1967).

5. W. S. Bickel, Appl. Opt. 6, 1309 (1967); J. A. Jordan, Jr., Ref. 3, pp. 121-156; S. Bashkin, Appl. Opt. 7, 2341 (1968).

6. E. Fermi, Nuclear Physics, revised ed., (University of Chicago Press, 1950), pp. 36, 37; E. Segré, Nuclei and Particles, (Benjamin Press, 1964), pp. 39-42; N. F. Mott and H. S. W. Massey, The Theory of Atomic Collisions, (Oxford Press, 1965), pp. 467-475, 629.

7. R. L. Wax, W. Bernstein, Rev. Sci. Instrum. 38, 1612 (1967).

8. cf. J. H. Ormrod, H. E. Duckworth, Canad. J. Phys. 41, 1424 (1963).

9. P. Jacquinot, Rep. Prog. Phys. 23, 267 (1960).

10. G. Bakken and J. A. Jordan, Jr., J. Opt. Soc. Amer. 59, 486 (1969); G. Bakken, Ph.D. Dissertation, Rice University (1969); J. A. Jordan, Jr., Ref. 3, pp. 121-156.

Figure Captions

Fig. 1.   Section of axicon optical system: B = ion beam, F =

carbon foil; A = axicon (in the present experiments,

cut from a piece of fused silica); C = beam stop; L =

lens; S = circular aperture in the focal plane of L.   In

our experiments a beam collimator is placed between F and

A to prevent any part of the scattered accelerator beam

from striking A or L, and a pressure-scanned Fabry-Perot

spectrometer (see Ref. 3) analyzes the light transmitted

by S.

Fig. 2.   Details of a ray path in an axicon.   E represents an

emitting ion.   Left: section through an axicon area

element dA, which reflects a ray from E, and the beam axis.

Right: section through dA perpendicular to beam axis.

All rays contained in the cone having half-angle Θ pass

through the aperture S (see Fig. 1).   Only rays originating

in the beam volume within that cone can reflect from dA and

pass through S.   The ray emitted by E leaves the axicon at

angle $\theta = (\alpha^2 + \varphi^2)^{1/2}$ with a parallel to the beam through dA.

Fig. 3.   Wavelength distribution in the plane of the aperture S.

Left: the quantity $[1 - 4\,\Delta\lambda^2/\delta\lambda^2]^{-1/2}$, proportional to

I_θ (see Eqs. (1) and (3)).   Right: the quantity

$[1 - 4\,\Delta\lambda^2/\delta\lambda^2]^{1/2}$, proportional to I (Eq. (4)).

Fig. 4. Degradation of line shapes and intensities with increasing carbon foil thickness, as observed with an axicon source and a Fabry-Perot interferometer. The top scan in each column was obtained by directing H_β light, at $\lambda 4861\text{Å}$, from an external hydrogen Geissler tube through the aperture S, and pressure-scanning the interferometer in the customary way. Axicon length approximately 1.0 cm, $\Theta = 0.0125$ radian, beam thickness 1.6 mm. Left column: hydrogen H_β (λ_o 4861Å); incident ion beam: 0.4 microamperes of H_3^+ at 0.21 MeV. Right column: O II ($\lambda 4639$-4642Å, large peak, and $\lambda 4649\text{Å}$, small peak); ion beam 0.3 microamperes of O_2^+ at 1.03 MeV. Pressure and wavelength increase to the left. Scan rate: approximately 2 Å/min. The interferometer's free spectral range is about 16Å. For the H_β scan, the shifts of the beam source lines relative to the external source are due partly to second-order Doppler shift (approximately .5Å) and partly due to residual first-order shifts whose causes have not been identified. Small asymmetries are due to variations in scan rate.

Fig. 5. Variation of observed linewidth of H_β (full width at half-maximum) with H_3^+ beam energy, for different carbon foil thicknesses. The dotted line shows the total width expected on the basis of the diameter of aperture S alone (Eq. (1)).

Fig. 6. Approximate linewidths of H_β attributed to scattering in carbon foils vs. σ/E^2, σ = foil surface density, E = beam energy. The incident ion is H_3^+. The linewidths are calculated by the relation $\Delta\lambda_s^2 = (FWHM)^2 - 4 \beta^2 \Theta^2 \lambda_o^2 - 1\mathring{A}^2$, i.e., by subtracting in quadrature the effects due to finite aperture S and instrumental width (see Fig. 4). The solid lines show the expected behavior of $\Delta\lambda_s^2$ (Ref. 6 and Eq. (5)), neglecting reduced mass effects and small changes in the logarithmic quantity. Range of foil thicknesses: 5.6 - 26.6 $\mu g/cm^2$; range of energies: .07 - .24 MeV/atom.

B F A C L   S

Fig 1

Fig 2

$$\left[1 - \frac{4\Delta\lambda^2}{\delta\lambda^2}\right]^{-\frac{1}{2}}$$

$$\left[1 - \frac{4\Delta\lambda^2}{\delta\lambda^2}\right]^{\frac{1}{2}}$$

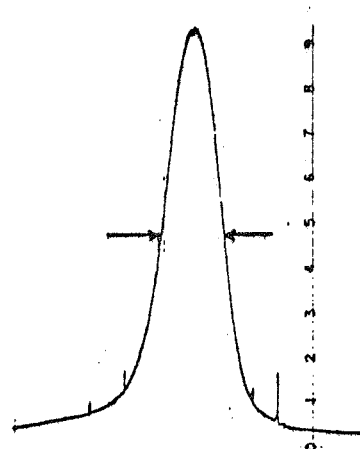$$\frac{2\Delta\lambda}{\delta\lambda} \longrightarrow$$
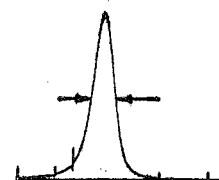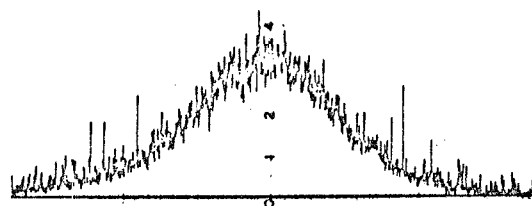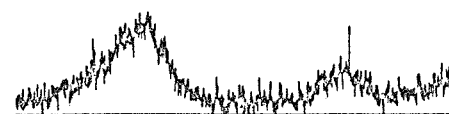
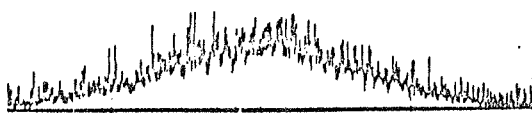$$\frac{2\Delta\lambda}{\delta\lambda} \longrightarrow$$
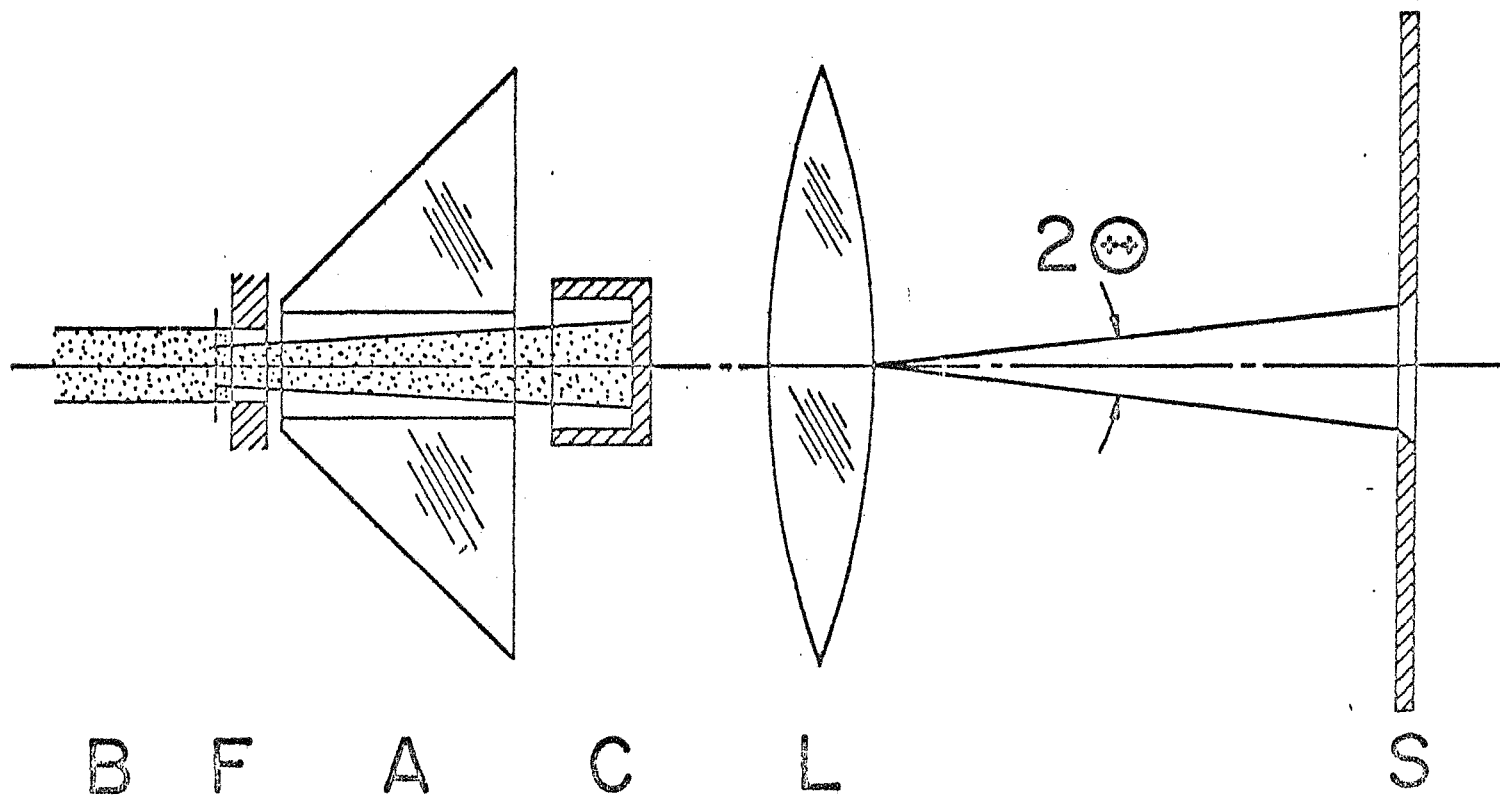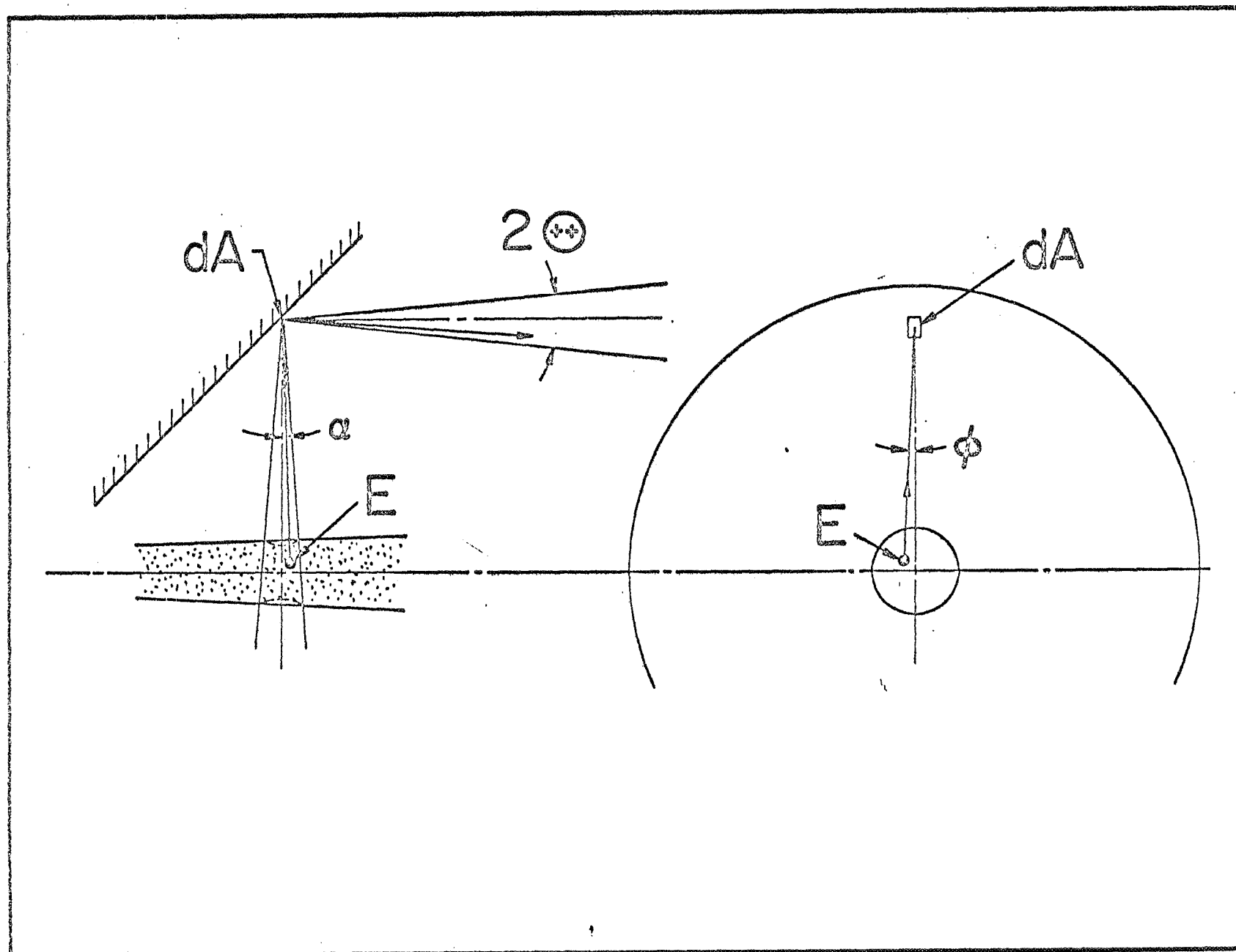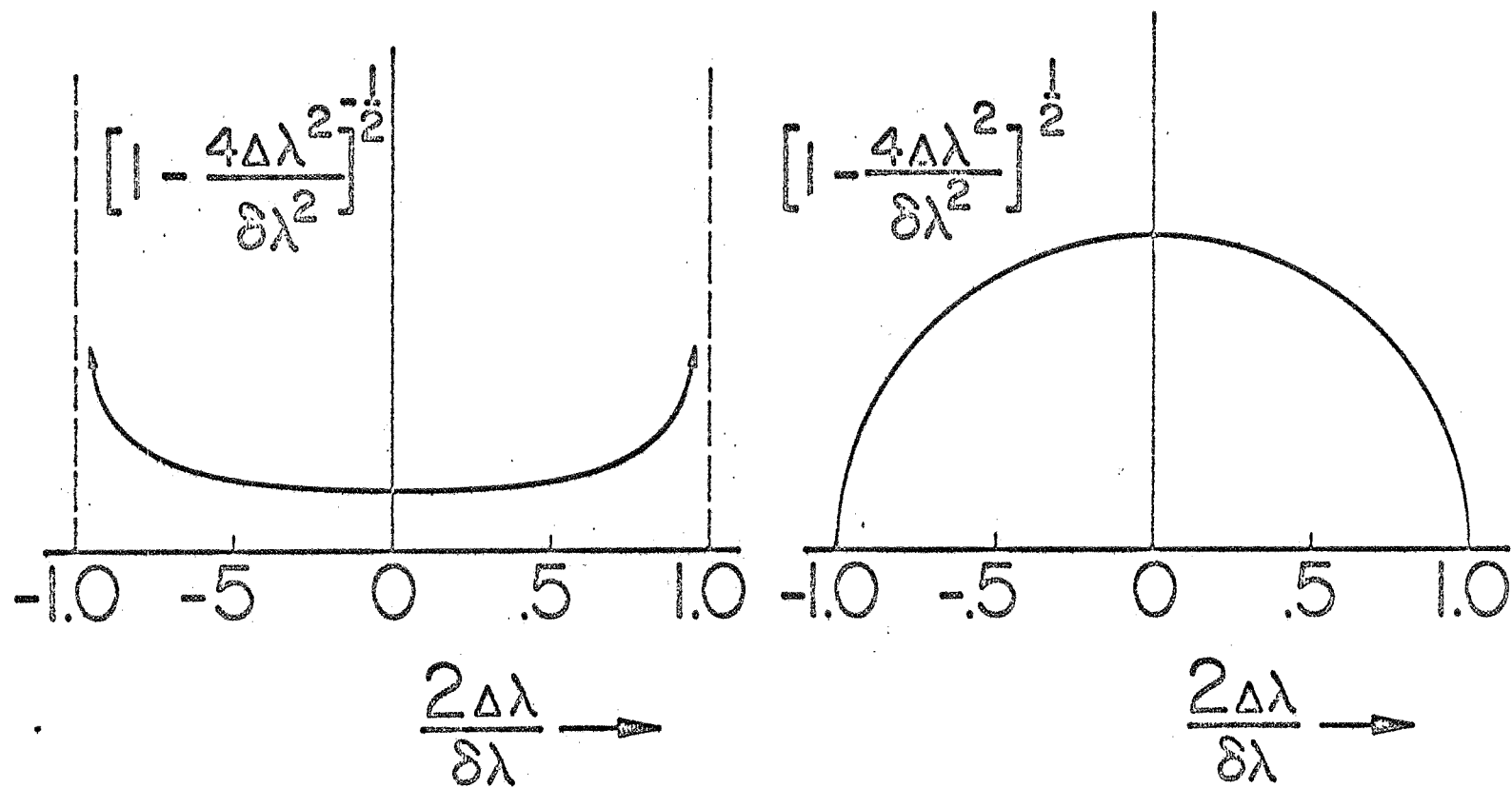
Fig 3

EXT. Hβ
SCAN
1.0Å FWHM
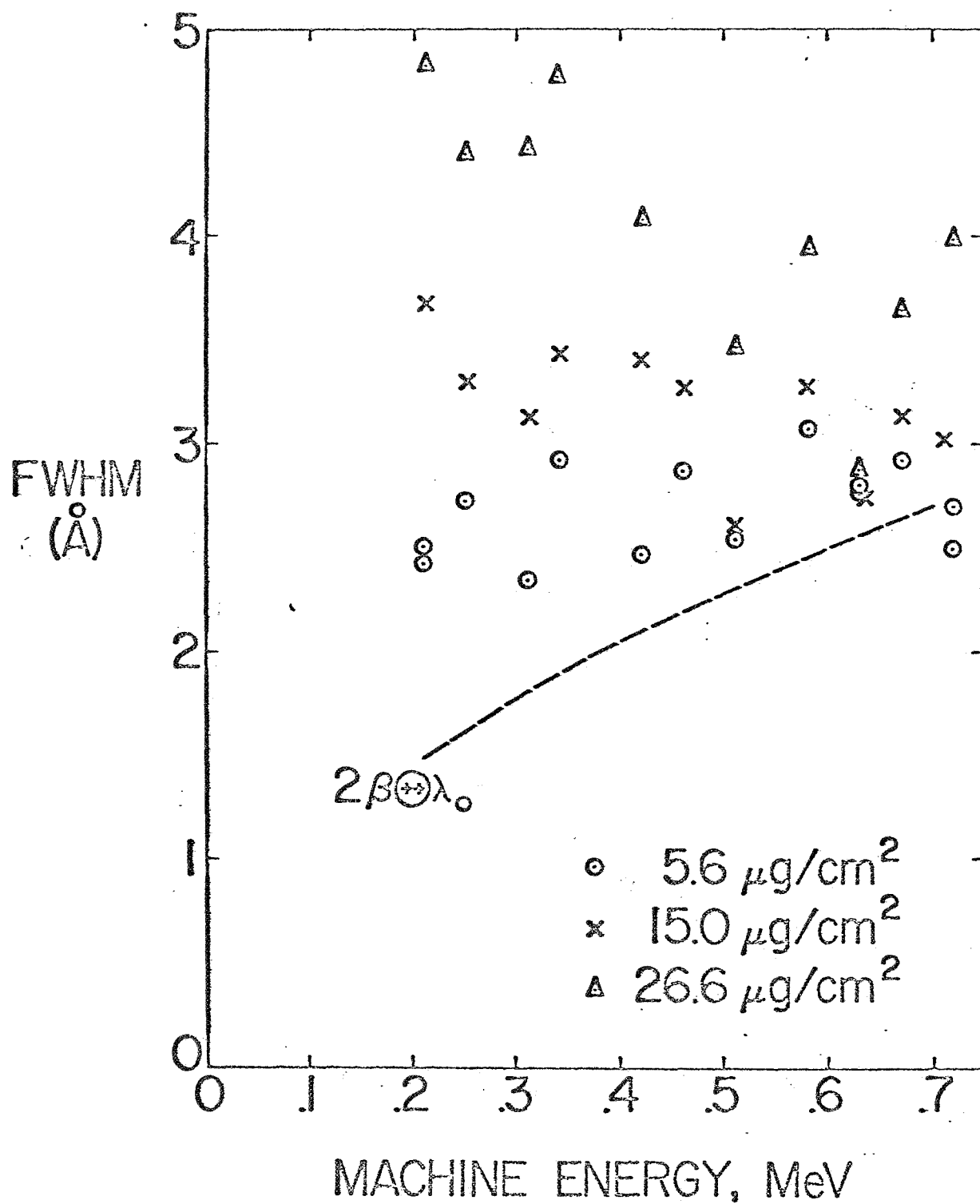
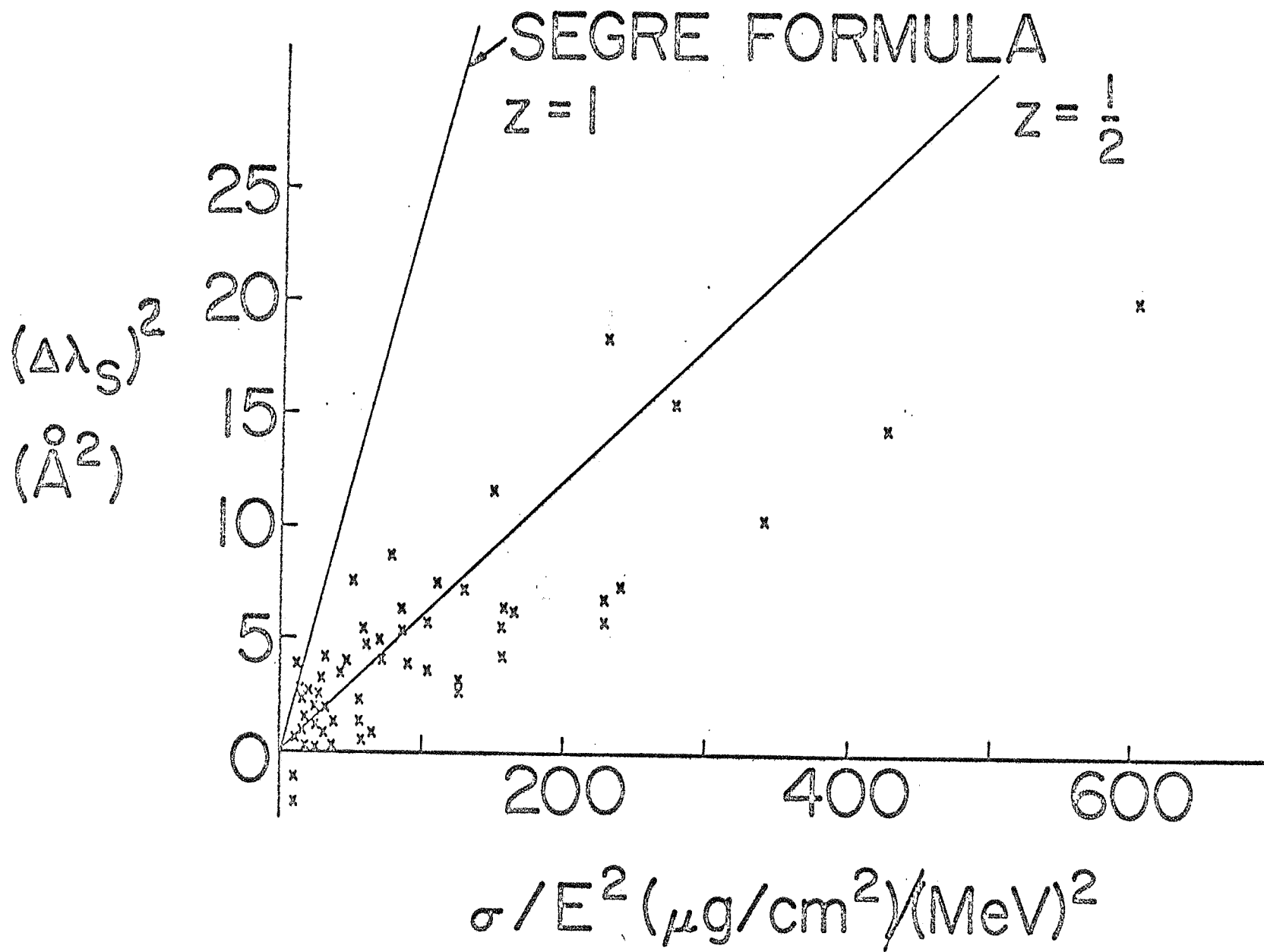BEAM SCANS

5.6

10.1

15.0

26.6

MICROGRAMS
CM²

Fig 4

FWHM (Å) vs MACHINE ENERGY, MeV

$2\beta \odot \lambda_o$

⊙ 5.6 μg/cm^2
✕ 15.0 μg/cm^2
△ 26.6 μg/cm^2

Fig 5

Fig 6